

On the Uncertainty Principle for Continuous Quantum Measurement

Haixing Miao¹

¹*School of Physics and Astronomy, University of Birmingham, Birmingham, B15 2TT, United Kingdom*

For continuous quantum measurements, there is a general Heisenberg uncertainty relation that constrains the quantum fluctuation of detectors with linear response, which is a generalization of the fluctuation-dissipation theorem to the scenarios far from thermal equilibrium. Here we show when the detector becomes ideal, i.e., having the minimum uncertainty, not only does the uncertainty relation takes the equal sign as expected, but also there are two new equalities. We illustrate the result by considering the typical cavity QED setup with the system, which the detector is coupled to, being either a qubit or a mechanical oscillator. Particularly, we look at the dispersive readout of qubit state, and the measurement of mechanical motional sideband asymmetry.

Introduction.—When we probe classical signals or quantum systems, noise in the detector limits our ability to extract the relevant information. If the classical noise is sufficiently suppressed, the detector will enter the regime where the intrinsic quantum fluctuation in its degrees of freedom determines the noise statistics. Modern experiments are approaching such a quantum-noise-limited regime [1, 2]. The state-of-the-art includes, e.g., high-fidelity qubit readout [3], laser interferometric gravitational-wave detection [4, 5], and quantum optomechanics in general [6, 7].

Most experiments mentioned above belong to the category of continuous linear quantum measurement, which is represented schematically in Fig. 1. The system can be, e.g., a qubit or a mechanical oscillator, which will be further attached to a classical signal if acting as a sensor. The detector is often a continuous quantum field that contains many degrees of freedom, e.g., the optical field in optomechanics. We call the degree of freedom linearly coupled to the system variable \hat{q} as the input port with its observable denoted by \hat{F} . Correspondingly, the output port with the observable \hat{Z} is the one projectively measured by a macroscopic device (e.g., the photodiode) that produces classical data.

The quantum fluctuation of \hat{Z} and \hat{F} gives rise to the so-called imprecision noise and the quantum back-action noise. These two types of quantum noise determines the performance of different measurement tasks. Even without knowing the detail of the detector and system, we can already set a general constraint on the quantum noise by applying the linear-response theory [8], which, according to Ref. [9], leads to the following Heisenberg uncertainty relation:

$$\bar{S}_{ZZ}(\omega)\bar{S}_{FF}(\omega) - |\bar{S}_{ZF}(\omega)|^2 \geq (\hbar^2/4)|\chi_{ZF}(\omega)|^2 + \hbar|\Im[\bar{S}_{ZF}^*(\omega)\chi_{ZF}(\omega) - \chi_{FF}(\omega)\bar{S}_{ZZ}(\omega)]|. \quad (1)$$

Here $\Im[\cdot]$ means taking the imaginary part; \bar{S} denotes the symmetrized spectral density [1], which quantifies the strength of the quantum fluctuation; χ is susceptibility that quantifies the detector response. Since the measurement process is far from thermal equilibrium, this relation generalizes the fluctuation-dissipation theorem [8, 10]. In the dispersive quantum non-demolition (QND) measurement of a qubit, \bar{S}_{ZZ} determines the measurement rate Γ_{meas} for acquiring the state information, and \bar{S}_{FF} sets the dephasing rate Γ_ϕ . This uncertainty relation leads to $\Gamma_{\text{meas}} \leq \Gamma_\phi$: we can measure the qubit at most

as fast as we dephase it [1, 11–14]. In the classical displacement or force sensing with a mechanical oscillator, Eq. (1) implies a tradeoff between the imprecision noise and the back-action noise, which gives rise to the Standard Quantum Limit (SQL) [9]. There are ongoing experimental efforts towards achieving the SQL and apply protocols to surpass it [6, 7], e.g., the most recent experimental results presented in Refs. [15–18]. Achieving the SQL requires the detector to be ideal, i.e., at the quantum limit with minimum uncertainty—the thermal excitation of the detector degrees of freedom and other decoherence effects become negligible.

Here we show that when the detector is at the quantum limit, not only do we have Eq. (1) attain the equal sign, but also obtain two new equalities shown in Eqs. (24) and (25). By introducing $\hat{z} \equiv \hat{Z}/\chi_{ZF}$ normalized by the response, they can be putted into the following more suggestive form:

$$\bar{S}_{zz}(\omega)\bar{S}_{FF}(\omega) - |\bar{S}_{zF}(\omega)|^2 = \frac{\hbar^2}{4}, \quad (2)$$

$$\Im[\bar{S}_{zF}(\omega)] = -\Im[\chi_{FF}(\omega)]\bar{S}_{zz}(\omega). \quad (3)$$

The first equality constraints the relative strength of the imprecision noise and the back-action noise, while the second one relates the cross correlation \bar{S}_{zF} to the dynamical back action quantified by χ_{FF} . To illustrate their implications, we apply them to the cavity QED setup. The key message goes as follows. In the case of dispersive qubit readout, we can find the optimal output observable such that $\bar{S}_{zF} = 0$, which leads to

$$\Gamma_{\text{meas}} = \Gamma_\phi. \quad (4)$$

In the case of measuring mechanical oscillator, we look at the motional sideband asymmetry reported in several experiments [19–23]. One interpretation is attributing the observed asymmetry to the imprecision-back-action noise correlation \bar{S}_{zF} [20, 24]. In particular, near the mechanical resonant frequency ω_m , \bar{S}_{zF} is purely imaginary and

$$\bar{S}_{zF}(\omega_m) \approx \pm i\hbar/2, \quad (5)$$



FIG. 1. A schematics for the continuous linear measurement.

where \pm depends on the detuning frequency of the laser. From Eqs. (2) and (3), such a correlation implies

$$\Im[\chi_{FF}(\omega_m)] \approx \mp \bar{S}_{FF}(\omega_m)/\hbar. \quad (6)$$

Firstly, this indicates that the noise spectra for the positive and negative frequencies are highly unbalanced, cf., Eq. (15), which is the case in these experiments. Secondly, χ_{FF} quantifies the dynamical back action which modifies the dynamics of the mechanical oscillator [25–27]; therefore, in linear measurements, the sideband asymmetry is always accompanied by additional heating or damping of the mechanical motion.

Definitions.—We now go through the mathematical description of the continuous linear measurement, and define relevant quantities, which follows Refs. [1, 9, 25]. Specifically, the free Hamiltonian \hat{H}_{det} of the detector only involves linear or quadratic functions of canonical coordinates of which the commutators are classical numbers. The system-detector interaction \hat{H}_{int} is in the bilinear form:

$$\hat{H}_{\text{int}} = -\hat{q}\hat{F}. \quad (7)$$

Solving the Heisenberg equation of motion leads to the following solution to the detector observables:

$$\hat{Z}(t) = \hat{Z}^{(0)}(t) + \int_{-\infty}^{+\infty} dt' \chi_{ZF}(t-t') \hat{q}(t'), \quad (8)$$

$$\hat{F}(t) = \hat{F}^{(0)}(t) + \int_{-\infty}^{+\infty} dt' \chi_{FF}(t-t') \hat{q}(t'), \quad (9)$$

where superscript (0) denotes evolution under the free Hamiltonian \hat{H}_{det} . The susceptibility χ_{AB} , quantifying the detector response to the system variable \hat{q} , is defined as

$$\chi_{AB}(t-t') \equiv (i/\hbar)[\hat{A}^{(0)}(t), \hat{B}^{(0)}(t')]\Theta(t-t'), \quad (10)$$

where Θ is the Heaviside function and we have assumed \hat{H}_{det} is time-independent so that χ_{AB} is a function of the time difference $t-t'$. Note that χ_{AB} is not an operator but a classical number, and it only depends on the free evolution of the detector; both features are attributable to the detector being linear. Moving into the frequency domain, we can relate the susceptibility to the spectral density:

$$\chi_{AB}(\omega) - \chi_{BA}^*(\omega) = (i/\hbar)[S_{AB}(\omega) - S_{BA}(-\omega)]. \quad (11)$$

Here S_{AB} is unsymmetrized spectral density defined through

$$\text{Tr}[\hat{\rho}_{\text{det}} \hat{A}^{(0)}(\omega) \hat{B}^{(0)}(\omega')] \equiv 2\pi S_{AB}(\omega) \delta(\omega - \omega'), \quad (12)$$

where $\hat{\rho}_{\text{det}}$ is the density matrix of the detector initial state, the Fourier transform $f(\omega) \equiv \int_{-\infty}^{+\infty} dt e^{i\omega t} f(t)$, and we have assumed $\text{Tr}[\hat{\rho}_{\text{det}} \hat{A}^{(0)}] = \text{Tr}[\hat{\rho}_{\text{det}} \hat{B}^{(0)}] = 0$ without loss of generality. The symmetrized version of S_{AB} , quantifying the fluctuation, is

$$\bar{S}_{AB}(\omega) \equiv [S_{AB}(\omega) + S_{BA}(-\omega)]/2. \quad (13)$$

One special case is when \hat{A} and \hat{B} are identical, which leads to Kubo's formula, using $\hat{A} = \hat{B} = \hat{F}$ as an example:

$$\Im[\chi_{FF}(\omega)] = [S_{FF}(\omega) - S_{FF}(-\omega)]/(2\hbar), \quad (14)$$

which quantifies the dissipation. In the thermal equilibrium, $S_{FF}(\omega)$ and $S_{FF}(-\omega)$ differ from each other by the Boltzmann factor $e^{\hbar\omega/(k_B T)}$ with T being temperature, and $\bar{S}_{FF}(\omega)$ is thus related to $\Im[\chi_{FF}(\omega)]$ by the fluctuation-dissipation theorem. For the measurement process far from thermal equilibrium, we generally have

$$\bar{S}_{FF}(\omega) \geq \hbar |\Im[\chi_{FF}(\omega)]|, \quad (15)$$

in which the equal sign is achieved when either $S_{FF}(\omega)$ or $S_{FF}(-\omega)$ vanishes [9]. This relation constraints the quantum fluctuation in either \hat{Z} or \hat{F} individually; the uncertainty relation Eq. (1) connect both together.

Uncertainty relation.—After defining key quantities, we come to the derivation of Eq. (1) and our main results Eqs. (2) and (3). We follow the standard approach outlined in Ref. [9], but use unsymmetrized spectral density as the starting point, which allows us to directly show the condition for achieving the quantum limit. Define the following auxiliary operator:

$$\hat{Q} \equiv \int_{-\infty}^{+\infty} d\omega [\alpha^*(\omega) \hat{Z}^{(0)}(\omega) + \beta^*(\omega) \hat{F}^{(0)}(\omega)], \quad (16)$$

where α, β are some functions. The norm of \hat{Q} is positive definite, i.e., $\|\hat{Q}\|^2 \equiv \text{Tr}[\hat{\rho}_{\text{det}} \hat{Q} \hat{Q}^\dagger] \geq 0$, which, in terms of unsymmetrized spectral density, reads

$$\int_{-\infty}^{+\infty} d\omega [\alpha^*, \beta^*] \begin{bmatrix} S_{ZZ}(\omega) & S_{ZF}(\omega) \\ S_{ZF}^*(\omega) & S_{FF}(\omega) \end{bmatrix} \begin{bmatrix} \alpha \\ \beta \end{bmatrix} \geq 0. \quad (17)$$

It needs to be satisfied for arbitrary α and β , which implies

$$S_{ZZ}(\omega) S_{FF}(\omega) - |S_{ZF}(\omega)|^2 \geq 0. \quad (18)$$

Using Eqs. (11) and (13), we can rewrite it as

$$\{\bar{S}_{ZZ}(\omega) \pm \hbar \Im[\chi_{ZZ}(\omega)]\} \{\bar{S}_{FF}(\omega) \pm \hbar \Im[\chi_{FF}(\omega)]\} \geq |S_{ZF}(\omega) \pm \frac{\hbar}{2i} [\chi_{ZF}(\omega) - \chi_{FZ}^*(\omega)]|^2. \quad (19)$$

Here \pm comes from that Eq. (18) needs to be satisfied for both positive and negative frequencies.

In order for \hat{F} and \hat{Z} to be the input and output observables of the detector, the susceptibilities cannot take arbitrary value. Because the macroscopic device, illustrated in Fig. 1, needs to make projective measurement of \hat{Z} continuously in time, which produces a classical data stream. This means the final \hat{Z} after interacting with the system, shown in Eq. (8), can be precisely measured at different times, which happens only if

$$[\hat{Z}(t), \hat{Z}(t')] = 0 \quad \forall t, t'. \quad (20)$$

In Ref. [25], the authors called this as the condition of simultaneous measurability, and further showed that it implies $[\hat{Z}^{(0)}(t), \hat{Z}^{(0)}(t')] = [\hat{F}^{(0)}(t), \hat{Z}^{(0)}(t')]\Theta(t-t') = 0$, i.e.,

$$\chi_{ZZ}(\omega) = \chi_{FZ}(\omega) = 0. \quad (21)$$

Taking this into account, Eq. (19) leads to

$$\bar{S}_{ZZ}(\omega)\bar{S}_{FF}(\omega) - |\bar{S}_{ZF}(\omega)|^2 \geq \frac{\hbar^2}{4}|\chi_{ZF}(\omega)|^2 \pm \hbar\Im[\bar{S}_{ZF}^*(\omega)\chi_{ZF}(\omega) - \chi_{FF}(\omega)\bar{S}_{ZZ}(\omega)]. \quad (22)$$

Since the inequality has to be valid for both plus sign and minus sign in front of $\hbar\Im[\cdot]$, it becomes equivalent to the uncertainty relation Eq. (1). Similar derivation is also presented in Ref. [1]; however, χ_{FF} has not been included, and this makes the resulting uncertainty relation less tight particularly when $\bar{S}_{ZF} \equiv \bar{S}_{ZF}/\chi_{ZF}$ becomes purely imaginary, as in the measurement of motional sideband asymmetry, cf., Eq. (5).

Detector at the quantum limit.—When the detector is at the quantum limit, Eq. (18) takes the minimum, i.e.,

$$\{S_{ZZ}(\omega)S_{FF}(\omega) - |S_{ZF}(\omega)|^2\}_{\text{quantum limit}} = 0. \quad (23)$$

Equivalently, this gives rise to two equalities for either plus sign or minus sign in Eq. (22). Taking their sum and difference, we obtain

$$\bar{S}_{ZZ}(\omega)\bar{S}_{FF}(\omega) - |\bar{S}_{ZF}(\omega)|^2 = \frac{\hbar^2}{4}|\chi_{ZF}(\omega)|^2, \quad (24)$$

$$\Im[\bar{S}_{ZF}^*(\omega)\chi_{ZF}(\omega) - \chi_{FF}(\omega)\bar{S}_{ZZ}(\omega)] = 0, \quad (25)$$

which are reduced to Eqs. (2) and (3) after normalizing \hat{Z} by the susceptibility χ_{ZF} .

We now show explicitly that the quantum limit is achieved when the detector is in the pure, stationary, Gaussian state—the multi-mode squeezed state (see, e.g., Ref. [28]):

$$|\xi\rangle \equiv \exp\left\{\int_0^{+\infty} \frac{d\omega}{2\pi} [\xi(\omega)\hat{d}^\dagger(\omega)\hat{d}^\dagger(-\omega) - \text{h.c.}]\right\} |0\rangle. \quad (26)$$

Here $\hat{d}(\omega)$ is the annihilation operator of the detector mode at frequency ω ; $\xi(\omega)$ describes the squeezing factor at different frequencies; h.c. denotes Hermitian conjugate; $|0\rangle$ is the vacuum state. In quantum optics, the zero frequency in Eq. (26) coincides with one half of the pump frequency of the optical parametric oscillator that produces the squeezed state.

Using the fact that $\hat{Z}^{(0)}(t)$ and $\hat{F}^{(0)}(t)$ are Hermitian, we can rewrite their Fourier transform in terms of $\hat{d}(\omega)$ and $\hat{d}^\dagger(-\omega)$:

$$\hat{Z}^{(0)}(\omega) = \mathcal{Z}(\omega)\hat{d}(\omega) + \mathcal{Z}^*(-\omega)\hat{d}^\dagger(-\omega), \quad (27)$$

$$\hat{F}^{(0)}(\omega) = \mathcal{F}(\omega)\hat{d}(\omega) + \mathcal{F}^*(-\omega)\hat{d}^\dagger(-\omega), \quad (28)$$

with some coefficients \mathcal{Z} and \mathcal{F} . One can then find that

$$\det \begin{bmatrix} \langle \xi | \hat{Z}(\omega) \hat{Z}^\dagger(\omega') | \xi \rangle & \langle \xi | \hat{Z}(\omega) \hat{F}^\dagger(\omega') | \xi \rangle \\ \langle \xi | \hat{F}(\omega) \hat{Z}^\dagger(\omega') | \xi \rangle & \langle \xi | \hat{F}(\omega) \hat{F}^\dagger(\omega') | \xi \rangle \end{bmatrix} = 0, \quad (29)$$

where the superscript (0) is omitted. This is equivalent to Eq. (23) according to the definition of the spectral density shown in Eq. (12).

Example.—We use the cavity QED setup shown schematically in Fig. 2 to illustrate the above result. The system can

either be a qubit or a mechanical oscillator. The detector consists of a single cavity mode \hat{a} and external continuum field \hat{c}_x with the central frequency defined by the laser frequency ω_l which could be detuned from the cavity resonant frequency ω_r . Its Hamiltonian in the rotating frame of the laser frequency is given by (see, e.g., section 2 in [6])

$$\hat{H}_{\text{det}} = \hbar(\omega_r - \omega_l)\hat{a}^\dagger\hat{a} - i\hbar \int_{-\infty}^{+\infty} dx \hat{c}_x^\dagger \frac{\partial \hat{c}_x}{\partial x} + i\hbar\sqrt{2\gamma}(\hat{a}^\dagger\hat{c}_{x=0} - \hat{a}\hat{c}_{x=0}^\dagger). \quad (30)$$

Here subscript x in \hat{c}_x labels the field degree of freedom at different locations; $\hat{c}_{x=0}$ denotes the one directly coupled to the cavity mode at a rate γ . This is the same Hamiltonian for a one-sided cavity in the standard input-output (has a different meaning from ours) formalism [29].

The interaction Hamiltonian in two cases, with the system to be a qubit (dispersive-coupling regime [30, 31]) and a mechanical oscillator (optomechanical coupling [6, 7]), are

$$\hat{H}_{\text{int}}^{\text{qubit}} = -\hbar \frac{g_0^2}{\omega_l - \omega_{01}} \hat{\sigma}_z \hat{a}^\dagger \hat{a}, \quad \hat{H}_{\text{int}}^{\text{mech}} = -\hbar \frac{\omega_r}{L} \hat{q}_m \hat{a}^\dagger \hat{a}, \quad (31)$$

where g_0 is the cavity-qubit coupling rate in the Jaynes-Cummings model, ω_{01} is the transition frequency between two energy levels, $\hat{\sigma}_z$ is the Pauli operator, L is the cavity length, and \hat{q}_m is the position of the mechanical oscillator.

For both cases, the input observable \hat{F} is proportional to the cavity photon number $\hat{n}_{\text{cav}} = \hat{a}^\dagger \hat{a}$ by comparing with Eq. (7), and thus in general we can write $\hat{F} = \hbar g \hat{n}_{\text{cav}}$ with g depending on the specific system. Due to pumping from the laser,

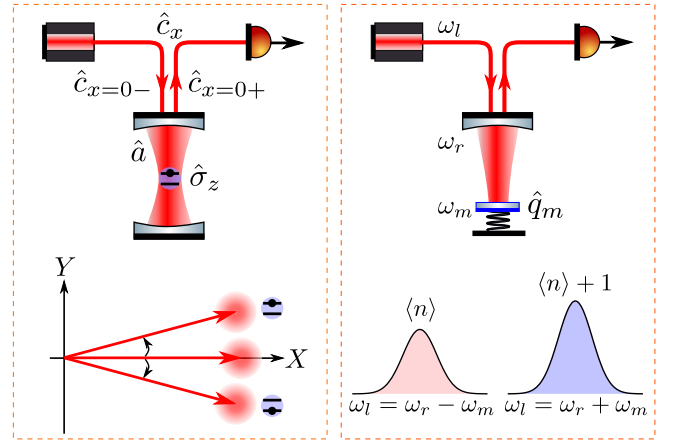


FIG. 2. Schematics for the dispersive qubit readout (left) in which the state-dependent phase shift is inferred by probing the phase quadrature \hat{Y} , and the sideband asymmetry measurement (right) in which we tune the laser frequency to selectively measure the Stokes and anti-Stokes sidebands scattered by the mechanical motion. In both cases, the cavity mode \hat{a} is continuously driven by the external field \hat{c}_x , which contains both the coherent amplitude and quantum fluctuation. We use $\hat{c}_{x=0-}$ ($\hat{c}_{x=0+}$) to denote the ingoing (outgoing) field right before (after) interacting with the cavity mode. The outgoing part is monitored by a photodiode using homodyne detection.

the mean cavity photon number \bar{n}_{cav} is much larger than one. The standard approach is linearizing \hat{n}_{cav} and keeping the perturbed part that is proportional to the amplitude quadrature $\hat{X} \equiv (\hat{a} + \hat{a}^\dagger)/\sqrt{2}$. The resulting linearized \hat{F} reads

$$\hat{F} = \hbar g \sqrt{2\bar{n}_{\text{cav}}} \hat{X} \equiv \hbar \bar{g} \hat{X}. \quad (32)$$

Additionally, given homodyne detection of the outgoing field $\hat{c}_{x=0+}$, the output observable \hat{Z} can be written as

$$\hat{Z} = \cos \theta \hat{X}_{\text{out}} + \sin \theta \hat{Y}_{\text{out}}, \quad (33)$$

where θ depends on the local oscillator phase, $\hat{X}_{\text{out}} \equiv (\hat{c}_{x=0+} + \hat{c}_{x=0+}^\dagger)/\sqrt{2}$ and $\hat{Y}_{\text{out}} \equiv (\hat{c}_{x=0+} - \hat{c}_{x=0+}^\dagger)/(\sqrt{2}i)$ are the amplitude quadrature and phase quadrature of the outgoing field.

To derive the susceptibilities and spectral densities, cf., Eqs. (10) and (12), we only need to solve the Heisenberg equation for the cavity mode and external field under the free evolution of \hat{H}_{det} , according to Ref. [29]:

$$\dot{\hat{a}}(t) = -(\gamma - i\Delta)\hat{a}(t) + \sqrt{2\gamma}\hat{c}_{x=0-}(t), \quad (34)$$

$$\dot{\hat{c}}_{x=0+}(t) = \hat{c}_{x=0-}(t) - \sqrt{2\gamma}\hat{a}(t), \quad (35)$$

where $\Delta \equiv \omega_l - \omega_r$ is the laser detuning frequency with respect to the cavity resonance. Solving these equations in the frequency domain, we can represent the cavity mode \hat{a} and the outgoing field $\hat{c}_{x=0+}$ in terms of the ingoing field $\hat{c}_{x=0-}$.

Without external squeezing, the spectral density for $\hat{c}_{x=0-}$ is simply $S_{\hat{c}\hat{c}^\dagger}(\omega) = 1$ (vacuum fluctuation) and $S_{\hat{c}^\dagger\hat{c}}(\omega) = 0$, from which we obtain the relevant spectra (double-sided):

$$\bar{S}_{ZZ}(\omega) = \frac{1}{2}, \quad (36)$$

$$\bar{S}_{ZF}(\omega) = \frac{\hbar \bar{g} \sqrt{\gamma} [\Delta \sin \theta - (i\omega - \gamma) \cos \theta]}{(\omega - \Delta + i\gamma)(\omega + \Delta + i\gamma)}, \quad (37)$$

$$\bar{S}_{FF}(\omega) = \frac{2\hbar^2 \bar{g}^2 \gamma (\gamma^2 + \Delta^2 + \omega^2)}{[(\omega - \Delta)^2 + \gamma^2][(\omega + \Delta)^2 + \gamma^2]}, \quad (38)$$

and the susceptibilities:

$$\chi_{ZF}(\omega) = -\frac{2\bar{g}\sqrt{\gamma}[\Delta \cos \theta + (i\omega - \gamma) \sin \theta]}{(\omega - \Delta + i\gamma)(\omega + \Delta + i\gamma)}, \quad (39)$$

$$\chi_{FF}(\omega) = \frac{2\hbar \bar{g}^2 \Delta}{(\omega - \Delta + i\gamma)(\omega + \Delta + i\gamma)}, \quad (40)$$

which satisfy Eqs. (24) and (25).

For the qubit readout, by introducing $\hat{z} \equiv \hat{Z}/\chi_{ZF}$, we have

$$\hat{z}(\omega) = \hat{z}^{(0)}(\omega) + \hat{\sigma}_z \delta(\omega). \quad (41)$$

Here we have used the fact that $\hat{\sigma}_z$ is a QND observable and remains constant in time. Therefore, the output responds to the signal only near DC with $\omega = 0$. For measurement with a finite duration, the delta function $\delta(\omega)$ is approximately given by the integration time. The measurement rate is defined by the inverse of the integration time that is required to reach

signal-to-noise ratio equal to one half, using the convention in Ref. [1]:

$$\Gamma_{\text{meas}} \equiv 1/[2S_{ZZ}(0)]. \quad (42)$$

The fluctuation in the cavity photon number induces a random AC Stark shift on the energy level, which causes dephasing, cf., Eq. (31). With measurement much longer than the cavity storage time, only the low-frequency part of the back-action noise spectrum is relevant, and according to Ref. [1], the dephasing rate is

$$\Gamma_\phi \equiv (2/\hbar^2) \bar{S}_{ZF}(0). \quad (43)$$

At the quantum limit, the ratio between these two rates is given by, cf., Eqs. (2), (37), and (39),

$$\frac{\Gamma_\phi}{\Gamma_{\text{meas}}} = 1 + \frac{4\bar{S}_{ZF}^2(0)}{\hbar^2} = 1 + \left(\frac{\Delta \sin \theta + \gamma \cos \theta}{\Delta \cos \theta - \gamma \sin \theta} \right)^2. \quad (44)$$

The optimal readout quadrature for reaching $\Gamma_\phi = \Gamma_{\text{meas}}$ is therefore the one satisfying

$$\theta_{\text{opt}} = -\arctan(\gamma/\Delta). \quad (45)$$

When the cavity is tuned with $\Delta = 0$, $\theta_{\text{opt}} = \pm\pi/2$ and the output phase quadrature is the optimal one, cf., Eq. (33), while for a large detuning $\Delta \gg \gamma$, $\theta_{\text{opt}} \approx 0$ and we need to measure the output amplitude quadrature. This result can be generalized to more complicated setups with, e.g., multiple coupled cavities. Because such a measurement is near DC and $\bar{S}_{ZF}(0)$ is real, we can always find the right readout quadrature such that $\bar{S}_{ZF}(0) = 0$, which makes $\Gamma_\phi = \Gamma_{\text{meas}}$ at the quantum limit.

We switch to the case of measuring mechanical motion. In contrast to the qubit readout, the position \hat{q}_m of the mechanical oscillator is not a QND observable, and the back-action noise will appear in the output:

$$\begin{aligned} \hat{z}(\omega) &= \hat{z}^{(0)}(\omega) + \hat{q}_m(\omega) \\ &= \hat{z}^{(0)}(\omega) + \chi_{qq}(\omega) [\hat{F}^{(0)}(\omega) + \hat{F}_{\text{th}}(\omega)], \end{aligned} \quad (46)$$

where we have used the fact that $\hat{q}_m = \chi_{qq}[\hat{F}^{(0)} + \hat{F}_{\text{th}}]$ and χ_{qq} is the mechanical susceptibility and \hat{F}_{th} the thermal Langevin force. Note that, more accurately, χ_{qq} should be replaced by $\chi_{qq}/[1 - \chi_{qq}\chi_{FF}]$ with the dynamical back action included, which however does not change the picture. The total output spectrum then reads

$$\bar{S}_{zz}^{\text{tot}}(\omega) = \bar{S}_{zz}(\omega) + 2\Re[\chi_{qq}^*(\omega)\bar{S}_{ZF}(\omega)] + \bar{S}_{qq}(\omega), \quad (47)$$

where $\Re[\cdot]$ means taking the real part. According to Refs. [20, 24], it is the second term, i.e., the cross correlation between the imprecision noise and the back-action noise, gives rise to the asymmetry. From Eqs. (37) and (39), we have

$$\bar{S}_{ZF}(\omega) = -\frac{\hbar}{2} \left[\frac{\Delta \sin \theta - (i\omega - \gamma) \cos \theta}{\Delta \cos \theta + (i\omega - \gamma) \sin \theta} \right]. \quad (48)$$

The experiments [19–23] are operating in the resolved side-band regime with $\gamma \ll \omega_m$ and having the detuning frequency $\Delta = \pm \omega_m$. Therefore, near the mechanical resonant frequency ω_m , \bar{S}_{zF} is approximately equal to the one shown in Eq. (5), which leads to

$$2\Re[\chi_{qq}^*(\omega_m)\bar{S}_{zF}(\omega_m)]|_{\Delta=\pm\omega_m} \approx \pm\hbar\Im[\chi_{qq}(\omega_m)]. \quad (49)$$

Since $\bar{S}_{qq}(\omega_m) = \hbar(2\langle n \rangle + 1)\Im[\chi_{qq}(\omega_m)]$ with the mean occupation number $\langle n \rangle = 1/(e^{\hbar\omega_m/k_B T} - 1)$ from the fluctuation-dissipation theorem, the above term either doubles or cancels the contribution from the zero-point fluctuation of the mechanical oscillator, which induces the observed asymmetry. According to Eq. (3), such an imaginary correlation is always associated with the dynamical back action that induces heating or damping of the mechanical motion:

$$\Im[\chi_{FF}(\omega_m)]_{\Delta=\pm\omega_m} \approx \mp\hbar\bar{g}^2/\gamma \approx \mp\bar{S}_{FF}(\omega_m)/\hbar, \quad (50)$$

as mentioned earlier in Eq. (6).

Before leaving this example, there is one comment motivated by Ref. [32]. The imaginary cross correlation is only detectable near the mechanical resonance when using the homodyne readout, because $\chi_{qq}(\omega_m)$ is also imaginary, which makes the second term in Eq. (47) nonzero. If measuring far away from the resonance or the oscillator were lossless, we will need to apply the synodyne readout scheme presented in Ref. [32] to probe such a quantum correlation.

Discussion.—We only cover the linear detectors with single input and single output, which is the case for most experiments mentioned above. The result can be generalized to multiple-input-multiple-output (MIMO) detectors through the following identity, which is a generalization of Eq. (29),

$$\det\langle\xi|\hat{A}(\omega)\hat{A}^\dagger(\omega')|\xi\rangle = 0, \quad (51)$$

where $\hat{A}^\dagger = (\hat{Z}_1^{(0)}, \hat{F}_1^{(0)}, \dots, \hat{Z}_N^{(0)}, \hat{F}_N^{(0)})^\dagger$ with N being the number of ports, and the condition of simultaneous measurability:

$$[\hat{Z}_k(t), \hat{Z}_l(t')] = 0 \quad \forall t, t' \quad (52)$$

with $k, l = 1, \dots, N$. This follows the same line as deriving the uncertainty relation for MIMO detectors and obtaining Eq. (1) as one special case in Ref. [9].

Acknowledgement.—H.M. would like to thank Farid Khalili and Yanbei Chen for important comments and discussions. This research is supported by EU Marie-Curie Fellowship and UK STFC Ernest Rutherford Fellowship.

[1] A. A. Clerk, M. H. Devoret, S. M. Girvin, F. Marquardt, and R. J. Schoelkopf, *Rev. Mod. Phys.* **82**, 1155 (2010).
[2] V. Giovannetti, S. Lloyd, and L. Maccone, *Nature Photonics* **5**, 222 (2011).
[3] E. Jeffrey, D. Sank, J. Y. Mutus, T. C. White, J. Kelly, R. Barends, Y. Chen, Z. Chen, B. Chiaro, A. Dunsworth,

A. Megrant, P. J. J. O'Malley, C. Neill, P. Roushan, A. Vainsencher, J. Wenner, A. N. Cleland, and J. M. Martinis, *Phys. Rev. Lett.* **112**, 190504 (2014).
[4] S. L. Danilishin and F. Y. Khalili, *Living Reviews in Relativity* **15** (2012).
[5] R. X. Adhikari, *Rev. Mod. Phys.* **86**, 121 (2014).
[6] Y. Chen, *Journal of Physics B: Atomic, Molecular and Optical Physics* **46**, 104001 (2013).
[7] M. Aspelmeyer, T. J. Kippenberg, and F. Marquardt, *Rev. Mod. Phys.* **86**, 1391 (2014).
[8] R. Kubo, *Reports on Progress in Physics* **29**, 255 (1966).
[9] V. B. Braginsky and F. Khalili, *Quantum Measurement* (Cambridge University Press, 1992).
[10] H. B. Callen and T. A. Welton, *Phys. Rev.* **83**, 34 (1951).
[11] D. V. Averin, *Physica C: Superconductivity and its Applications* **352**, 120 (2001).
[12] S. Pilgram and M. Büttiker, *Phys. Rev. Lett.* **89**, 200401 (2002).
[13] D. V. Averin, *arXiv:cond-mat/0301524* (2003).
[14] A. A. Clerk, S. M. Girvin, and A. D. Stone, *Phys. Rev. B* **67**, 165324 (2003).
[15] J. B. Clark, F. Lecocq, R. W. Simmonds, J. Aumentado, and J. D. Teufel, *Nature Physics* **12**, 683 (2016).
[16] C. U. Lei, A. J. Weinstein, J. Suh, E. E. Wollman, A. Kronwald, F. Marquardt, A. A. Clerk, and K. C. Schwab, *arXiv:1605.08148* (2016).
[17] T. P. Purdy, K. E. Grutter, K. Srinivasan, and J. M. Taylor, *arXiv:1605.05664* (2016).
[18] V. Sudhir, R. Schilling, S. A. Fedorov, H. Schuetz, D. J. Wilson, and T. J. Kippenberg, *arXiv:1608.00699* (2016).
[19] A. H. Safavi-Naeini, J. Chan, J. T. Hill, T. P. M. Alegre, A. Krause, and O. Painter, *Phys. Rev. Lett.* **108**, 033602 (2012).
[20] A. J. Weinstein, C. U. Lei, E. E. Wollman, J. Suh, A. Metelmann, A. A. Clerk, and K. C. Schwab, *Physical Review X* **4**, 041003 (2014).
[21] T. P. Purdy, P. L. Yu, N. S. Kampel, R. W. Peterson, K. Cicak, R. W. Simmonds, and C. A. Regal, *Phys. Rev. A* **92**, 031802(R) (2015).
[22] M. Underwood, D. Mason, D. Lee, H. Xu, L. Jiang, A. B. Shkarin, K. Børkje, S. M. Girvin, and J. G. E. Harris, *Phys. Rev. A* **92**, 061801 (2015).
[23] V. Sudhir, D. J. Wilson, R. Schilling, H. Schütz, S. A. Fedorov, A. H. Ghadimi, A. Nunnenkamp, and T. J. Kippenberg, *arXiv:1602.05942* (2016).
[24] F. Y. Khalili, H. Miao, H. Yang, A. H. Safavi-Naeini, O. Painter, and Y. Chen, *Phys. Rev. A* **86**, 033840 (2012).
[25] A. Buonanno and Y. Chen, *Phys. Rev. D* **65**, 042001 (2002).
[26] I. Wilson-Rae, N. Nooshi, W. Zwerger, and T. J. Kippenberg, *Phys. Rev. Lett.* **99**, 093901 (2007).
[27] F. Marquardt, J. P. Chen, A. A. Clerk, and S. M. Girvin, *Phys. Rev. Lett.* **99**, 093902 (2007).
[28] K. J. Blow, R. Loudon, S. J. D. Phoenix, and T. J. Shepherd, *Phys. Rev. A* **42**, 4102 (1990).
[29] C. W. Gardiner and M. J. Collett, *Phys. Rev. A* **31**, 3761 (1985).
[30] A. Blais, R. S. Huang, A. Wallraff, S. M. Girvin, and R. J. Schoelkopf, *Phys. Rev. A* **69**, 062320 (2004).
[31] A. Wallraff, D. I. Schuster, A. Blais, L. Frunzio, J. Majer, M. H. Devoret, S. M. Girvin, and R. J. Schoelkopf, *Phys. Rev. Lett.* **95**, 060501 (2005).
[32] L. F. Buchmann, S. Schreppler, J. Kohler, N. Spethmann, and D. M. Stamper-Kurn, *Phys. Rev. Lett.* **117**, 030801 (2016).